Chemical Geology 470 (2017) 152–163

Contents lists available at ScienceDirect

Chemical Geology

journal homepage: www.elsevier.com/locate/chemgeo

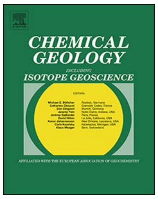

Manganese-calcium intermixing facilitates heteroepitaxial growth at the $(10\bar{1}4)$ calcite-water interface

Man Xu[a], Shawn L. Riechers[a], Eugene S. Ilton[a], Yingge Du[a], Libor Kovarik[b], Tamas Varga[b], Bruce W. Arey[c], Odeta Qafoku[a], Sebastien Kerisit[a,*]

[a] *Physical and Computational Sciences Directorate, Physical Sciences Division, Pacific Northwest National Laboratory, Richland, WA 99352, United States*
[b] *Earth and Biological Sciences Directorate, Environmental Molecular Sciences Division, Pacific Northwest National Laboratory, Richland, WA 99352, United States*
[c] *Energy and Environment Directorate, Nuclear Sciences Division, Pacific Northwest National Laboratory, Richland, WA 99352, United States*

ARTICLE INFO

Editor: J. Fein

Keywords:
Metal carbonates
Epitaxy
Mineral growth
Lattice mismatch
Mineral coatings

Abstract

In situ atomic force microscopy (AFM) measurements were performed to probe surface precipitates that formed on the $(10\bar{1}4)$ surface of calcite ($CaCO_3$) single crystals following reaction with Mn^{2+}-bearing aqueous solutions. Three-dimensional epitaxial islands were observed to precipitate and grow on the surfaces. In situ time-sequenced measurements demonstrated that the growth rates were commensurate with those obtained for epitaxial islands formed on calcite crystals reacted with Cd^{2+}-bearing aqueous solutions of the same range in supersaturation with respect to the pure metal carbonate phase. This finding was unexpected as rhodochrosite ($MnCO_3$) and calcite display a 10% lattice mismatch, based on the area of their $(10\bar{1}4)$ surface unit cells, whereas the lattice mismatch is only 4% for otavite ($CdCO_3$) and calcite. Coatings of varying thicknesses were therefore synthesized by reacting calcite single crystals in calcite-equilibrated aqueous solutions with up to 250 μM $MnCl_2$. Ex situ X-ray photoelectron spectroscopy (XPS), scanning transmission electron microscopy (STEM), energy-dispersive X-ray spectroscopy (EDX), X-ray diffraction (XRD), X-ray reflectivity (XRR), and AFM measurements of the reacted crystals demonstrated the formation of an epitaxial $(Mn,Ca)CO_3$ solid solution. The epitaxial solid solution had a spatially complex composition, whereby the first few nanometers were rich in Ca and the Mn content increased with distance from the original calcite surface, culminating in a topmost region of almost pure $MnCO_3$ for the thickest coatings. The effective lattice mismatch was therefore much smaller than the nominal mismatch thus explaining the measured growth rates. These findings highlight the strong influence played by the substrate on the composition of surface precipitates in aqueous conditions.

1. Introduction

Mineral/fluid interfaces are highly complex due, in part, to the formation of mineral coatings through heterogeneous nucleation and growth, which is a dominant pathway for mineral formation in aqueous systems. If similarities in atomic structure between the substrate and the growing phase allow for lattice registry, heteroepitaxial coatings with extensive surface coverage can develop, thereby altering, or eventually masking, the reactive properties of the substrate. Examples from the literature include oxide nanostructures grown on carbonate surfaces (Jun et al., 2005; Na and Martin, 2008, 2009) that were shown to exhibit vastly different electrostatic and van der Waals interfacial forces than their substrate, indicative of different surface charges, and heteroepitaxial metal carbonate overgrowths (Prieto et al., 2003; Pérez-Garrido et al., 2007; Pérez-Garrido et al., 2009) that extensively covered and blocked further dissolution of their calcium carbonate substrate, thereby preventing the solution from reaching equilibrium with respect to the carbonate phases.

Heteroepitaxial systems have been studied extensively in conditions pertinent to the growth of semiconductor thin films from the gas phase (Voigtländer, 2001). Growth mechanisms have been identified and categorized (Frank-Van der Meer, Stranski-Krastanov, and Volmer-Weber), and atomistic models have been developed for simple systems (Lam et al., 2008; Orr et al., 1992; Russo and Smereka, 2006), driven for the most part by the quest for controllable and tunable semiconductor nanostructures such as quantum dots (Springholz et al., 1998). In contrast, and despite evidence of heteroepitaxial growth in natural systems or simulated natural conditions, such as the growth of various phases on hydroxide (Ruiz-Agudo et al., 2013), silicate (Nagy et al., 1999; Lee et al., 2016), carbonate (Lea et al., 2003; Ruiz-Agudo

---

* Corresponding author.
E-mail address: sebastien.kerisit@pnnl.gov (S. Kerisit).

http://dx.doi.org/10.1016/j.chemgeo.2017.09.001
Received 22 April 2017; Received in revised form 30 August 2017; Accepted 1 September 2017

et al., 2016), and sulfate (Shtukenberg et al., 2005) mineral substrates, quantitative knowledge of the factors controlling the nucleation, growth rates, structure, and composition of epitaxial mineral coatings at mineral/water interfaces is still limited. This knowledge gap stems mostly from the multitude of reaction pathways that emerge in aqueous conditions as well as from the difficulties in detecting and probing epitaxial coatings due to their nanometer-scale dimensions, patchiness, and similarity of structure with their substrate. Addressing this knowledge gap is essential to have a robust understanding and ability to predict the behavior of geochemical systems. For example, several divalent toxic metals (Cd^{2+}, Pb^{2+}, Co^{2+}, etc.) (Xu et al., 1996; Chiarello et al., 1997; Chada et al., 2005) can form or be incorporated in carbonate coatings on calcium carbonate surfaces, a process that controls their mobility and bioavailability in the environment and can be exploited as a remediation strategy for polluted waters (Prieto et al., 2003). In another example, mineral trapping of CO_2 as carbonate minerals is both a natural process and one that offers a stable, long-term storage mechanism in the context of geologic carbon sequestration (Oelkers et al., 2008).

Previous work by our group (Xu et al., 2014, 2015; Riechers et al., 2017) and others (Pérez-Garrido et al., 2007; Chiarello et al., 1997; Stipp et al., 1992; Chiarello and Sturchio, 1994; Hay et al., 2003; Cubillas and Higgins, 2009; Callagon et al., 2017) has explored the heteroepitaxial nucleation and growth of otavite ($CdCO_3$) on calcite ($CaCO_3$), which are isostructural carbonates that display a 4% lattice mismatch, based on the area of their $(10\bar{1}4)$ surface unit cells. In particular, advancement of existing steps and nucleation and growth of three-dimensional islands were observed at low initial supersaturation, whereas nucleation and spread of two-dimensional nuclei were detected at high initial supersaturation; rates of growth were quantified for each mode (Xu et al., 2014). In contrast, similar experiments with Co^{2+}-bearing aqueous solutions did not yield any evidence of the formation of heteroepitaxial surface precipitates (Xu et al., 2015), which is consistent with the very large lattice mismatch between sphaerocobaltite ($CoCO_3$) and calcite (−15%).

The reaction of aqueous Mn^{2+} – another important carbonate-forming divalent cation – with calcite has been the subject of a number of studies stretching over several decades. Only studies performed in the heterogeneous growth regime, whereby the solution is not supersaturated with respect to calcite, will be reviewed here, i.e. not considering works related to Mn^{2+} incorporation during calcite growth. Early work (McBride, 1979; Franklin and Morse, 1983) showed that the interaction of Mn^{2+} with calcite followed a three-stage process: initial rapid adsorption, followed by a period of slower adsorption, during which $MnCO_3$ was thought to nucleate, and finally, for high initial Mn concentrations, growth of $MnCO_3$ at the surface. McBride (1979) used electron spin resonance (ESR) to show the formation of a Mn-containing carbonate phase at the surface of calcite powders following chemisorption. More recent AFM studies by Lea et al. (2003) and Pérez-Garrido et al. (2009) described the formation of rod-like three-dimensional islands during the reaction of aqueous Mn^{2+} with calcite single crystals. The morphologies were very similar to the heteroepitaxial islands formed in Cd^{2+}-bearing aqueous solutions, as discussed above. This finding is surprising as the lattice mismatch of rhodochrosite ($MnCO_3$) with respect to calcite (−10%) is much larger compared to otavite. Lea et al. (2003) suggested pseudokutnohorite (disordered $Mn_{0.5}Ca_{0.5}CO_3$) formed but neither study provided a robust determination of the surface precipitate composition. Additionally, the growth rate of the precipitates was either not explored (Pérez-Garrido et al., 2009) or only measured over a limited range of supersaturations (Lea et al., 2003). Importantly, it was also not compared to growth rates obtained for Cd^{2+}-reacted calcite crystals to extract the effect of the lattice mismatch, an important quantity when considering heterogeneous nucleation and growth (Jung et al., 2016; Jung and Jun, 2016). Indeed, the strain induced in the growing heteroepitaxial phase by the lattice mismatch reduces the supersaturation, which is expected to translate to higher equilibrium concentrations and, in turn, lower growth rates.

In this contribution, we systematically quantified the growth rates of precipitates observed on Mn^{2+}-reacted calcite single crystals using time-sequenced atomic force microscopy (AFM) measurements, and we compared the results to our previous work for Cd^{2+}-bearing aqueous solutions (Xu et al., 2014). Our working hypothesis heading into this study was that growth rates should show a dependence on the degree of lattice mismatch. However, the formation of a manganese-calcium carbonate solid solution could modify this hypothesis. In this regard, as is apparent from the above review of previous studies, a direct determination of the precipitate composition has been elusive. Consequently, we also employed a combination of X-ray photoelectron spectroscopy (XPS), scanning transmission electron microscopy (STEM), energy-dispersive X-ray spectroscopy (EDX), X-ray diffraction (XRD), and X-ray reflectivity (XRR) to unequivocally determine the composition of surface precipitates and any potential influence from the substrate.

2. Experimental methods

2.1. Materials and solutions

Calcite specimens used in this study were prepared from optically-clear calcite crystals (Ward's Natural Science Establishment, Inc.) sourced from Minas Gerais, Brazil. Fresh specimens were cleaved with a razor blade along the $(10\bar{1}4)$ cleavage plane minutes before performing the experiments. The specimens were handled with PTFE tweezers to avoid contamination and were cleaned with bursts of $N_2(g)$ to remove small particles from the surfaces. Aqueous solutions were prepared from high-purity $MnCl_2$ (anhydrous, 99.99%) or $CdCl_2$ (Aldrich, 99.99%) salts dissolved in deionized water (resistivity ~18 MΩ).

2.2. In Situ Experiments

The in situ AFM experiments were conducted at ~22 °C in a custom-built Kel-F cell with a diameter of 2.7 cm and a volume of approximately 2.5 mL. Following the approach used in our previous in situ AFM experiments of calcite in contact with $CdCl_2$ and $CoCl_2$ solutions (Xu et al., 2014, 2015), calcite specimens of approximately 10 mm × 12 mm × 1.5 mm in size were fixed in the fluid cell with Crystalbond (Crystalbond 509, SPI Supplies) by heating on a hot plate, cooled on an aluminum block for 5 min, and contacted with 2.3 mL of deionized water. After exactly 30 min, a small volume of a concentrated $MnCl_2$ solution was introduced to obtain specific initial concentrations of Mn^{2+}, denoted $[Mn^{2+}]_0$.

Two series of in situ AFM experiments were performed. In the first series, which was aimed at determining the morphology and nature of the surface precipitates, the calcite specimens were reacted under anoxic conditions in a glove box with $O_2 < 0.2$ ppm for 4 or 16 h following addition of $MnCl_2$ ($[Mn^{2+}]_0 = 10$, 25, 50, 100, and 200 μM for the 4-hour experiments, whereas the 16-hour experiments were limited to $[Mn^{2+}]_0 = 100$ and 200 μM). The fluid cell was then taken out of the glove box and 10 to 12 different areas of $6 \times 6\ \mu m^2$ to $15 \times 15\ \mu m^2$ in size were imaged by AFM directly in the reacting solutions. Duplicates of the 16-hour experiments were dried with pressurized $N_2(g)$ and analyzed with XPS, as described below. These samples were not stored in an inert-atmosphere container and were thus exposed to air before loading in the spectrometer.

In the second series of experiments, which was aimed at measuring the growth rates of surface precipitates, the fluid cell was taken out of the glove box 30 min after $MnCl_2$ addition and time-sequences of AFM images were then taken in the reacting solutions and in air for up to 5 h. Between 3 and 5 duplicate experiments were performed at each concentration to ensure consistency. An additional $MnCl_2$ concentration, 150 μM, was considered in this series and control experiments were also